4980 *Chem. Mater.* **2010,** *22,* 4980–4986
DOI:10.1021/cm1013152

CHEMISTRY OF MATERIALS
Article

Printable Nanoporous Silver Membranes

Norman A. Luechinger, Samuel G. Walt, and Wendelin J. Stark*

Institute for Chemical and Bioengineering, Department of Chemistry and Applied Biosciences, ETH Zurich, CH-8093 Zurich, Switzerland

Received May 10, 2010. Revised Manuscript Received July 22, 2010

We present a facile, broadly applicable method to prepare nanoporous silver films using soluble salt nanoparticles as pore templates. The fabrication starts by printing a silver/$CaCO_3$ nanoparticle based ink onto a flexible substrate and removing the $CaCO_3$ by washing in a weak acid. The membrane thickness and pore size can easily be tuned between 0.5−5 μm and 30−300 nm, respectively, by a simple pH or temperature treatment (sintering at 200 °C). As a conceptual demonstration of the resulting large-area, defect-free, and homogeneous microstructure, we use these membranes to efficiently filter aqueous dispersions of carbon nanoparticles (20 nm primary particle size) at a filtration efficiency of >99.6%.

Introduction

Nanoporous metals have attracted a tremendous interest during the last few years due to their unique characteristics in catalytic,[1,2] optical,[2] sensing,[3,4] and actuation[5] applications. The fabrication of nanoporous metals has been investigated using two approaches, templating and dealloying. Templating techniques utilize polymers,[6,7] carbon,[8] glass,[9] or liquid-crystals[10] as sacrificial pore templates. Dealloying starts from a metal alloy and introduces nanoporosity by selective etching of a certain alloy component. This process has been most successfully used to produce Raney metals for more than 80 years.[11] The evolution of nanoporosity in dealloyed metals has first been described by Erlebacher and co-workers.[12]

Although there are many possible templating methods for the production of nanoporous metals, most of them are limited to the fabrication of bulk or macroscopic geometries and are unsuitable to obtain thin, large area nanoporous metals. In contrast, dealloying gives access to porous membranes. Nanoporous gold leaf (NPGL) is one of the most prominent nanoporous metal membranes. It is prepared by dealloying and has been used in numerous studies owing to its facile production from gold leaf.[1,13−16] For most commercial applications, such as in fuel cell electrodes, gold is believed to be too expensive.[15] Silver would be a promising alternative material. Zhang et al. have demonstrated how to fabricate nanoporous silver membranes by cosputtering of Ag and Al with a subsequent dealloying step.[17] This fascinating method is very attractive to high value, small scale applications, as sputtering and the related fine vacuum processes are still rather expensive.

In this study, we present a facile, broadly applicable method to prepare nanoporous metal films using soluble salt nanoparticles as pore templates. One-step fabrication of the metal/salt composite nanoparticles circumvents potential particle mixing problems (unfavorable wetting of most metal/salt pairs).[18] We demonstrate the potential of salt pore templating by preparing large area, free-standing, crack-free silver membranes. As a conceptual demonstration of a potential technical application, we use these membranes to efficiently filter aqueous dispersions of carbon nanoparticles.

Experimental Section

Reagents and Materials. Ag-octanoate was purchased from Metalor, and Ca-2-ethylhexanoate was purchased from Molekula

*To whom correspondence should be addressed. Fax: +41 44 633 1083. E-mail: wstark@ethz.ch.

(1) Ge, X. B.; Wang, R. Y.; Liu, P. P.; Ding, Y. *Chem. Mater.* **2007**, *19*, 5827.
(2) Ding, Y.; Chen, M. W. *MRS Bull.* **2009**, *34*, 569.
(3) Yu, F.; Ahl, S.; Caminade, A. M.; Majoral, J. P.; Knoll, W.; Erlebacher, J. *Anal. Chem.* **2006**, *78*, 7346.
(4) Kucheyev, S. O.; Hayes, J. R.; Biener, J.; Huser, T.; Talley, C. E.; Hamza, A. V. *Appl. Phys. Lett.* **2006**, 89.
(5) Weissmuller, J.; Viswanath, R. N.; Kramer, D.; Zimmer, P.; Wurschum, R.; Gleiter, H. *Science* **2003**, *300*, 312.
(6) Dobrev, D.; Neumann, R.; Angert, N.; Vetter, J. *Appl. Phys. A: Mater. Sci. Process.* **2003**, *76*, 787.
(7) Velev, O. D.; Tessier, P. M.; Lenhoff, A. M.; Kaler, E. W. *Nature* **1999**, *401*, 548.
(8) Fischer, A.; Jun, Y. S.; Thomas, A.; Antonietti, M. *Chem. Mater.* **2008**, *20*, 7383.
(9) Masuda, H.; Nishio, K.; Baba, N. *J. Mater. Sci. Lett.* **1994**, *13*, 338.
(10) Ding, Y.; Mathur, A.; Chen, M. W.; Erlebacher, J. *Angew. Chem., Int. Ed.* **2005**, *44*, 4002.
(11) Raney, M., *U.S. Patent* 1,628,190 1927.
(12) Erlebacher, J.; Aziz, M. J.; Karma, A.; Dimitrov, N.; Sieradzki, K. *Nature* **2001**, *410*, 450.
(13) Ding, Y.; Kim, Y. J.; Erlebacher, J. *Adv. Mater.* **2004**, *16*, 1897.
(14) Zeis, R.; Lei, T.; Sieradzki, K.; Snyder, J.; Erlebacher, J. *J. Catal.* **2008**, *253*, 132.
(15) Zeis, R.; Mathur, A.; Fritz, G.; Lee, J.; Erlebacher, J. *J. Power Sources* **2007**, *165*, 65.
(16) Ciesielski, P. N.; Scott, A. M.; Faulkner, C. J.; Berron, B. J.; Cliffel, D. E.; Jennings, G. K. *ACS Nano* **2008**, *2*, 2465.
(17) Zhang, W. Y.; Li, Y. N.; Li, G. Z.; Wang, Q. B.; Tang, H. P.; Xi, Z. P.; Fang, M. In *Porous Metals and Metallic Foams: Metfoam 2007*; Lefebvre, L. P., Banhart, J., Dunand, D. C., Eds.; Metfoam 2007: Montreal, Canada, 2008; p 325.
(18) Grass, R. N.; Albrecht, T. F.; Krumeich, F.; Stark, W. J. *J. Mater. Chem.* **2007**, *17*, 1485.

Published on Web 08/10/2010

(4.5% in 2-ethylhexanoic acid). Xylene, HCl, dichloromethane, and dimethyl-sulfoxide were of analytical grade. The dispersant DB190 was obtained from BYK Chemie. The polymers Polysulfone (PSU) and Polyimide (Torlon 4000) were purchased in powder form.

Synthesis of $Ag/CaCO_3$ Nanoparticles. $Ag/CaCO_3$ nanoparticles were prepared by flame spray synthesis.[19] Ag-octanoate was mixed with Ca-2-ethylhexanoate (4.5% in 2-ethylhexanoic acid and finally diluted 2:1 (w/w) with xylene. The precursor then was fed (7 mL min^{-1}, HNP Mikrosysteme, micro annular gear pump mzr-2900) to a spray nozzle, dispersed by oxygen (7 L min^{-1}, PanGas Tech.), and ignited by a premixed methane−oxygen flame (CH_4, 1.2 L min^{-1}; O_2, 2.2 L min^{-1}).[19] The off-gas was filtered through a glass fiber filter (Schleicher & Schuell) by a vacuum pump (Busch, Seco SV1040CV) at about 20 m^3 h^{-1}.

Preparation of the $Ag/CaCO_3$ Dispersion. A water-based dispersion of the obtained $Ag/CaCO_3$ nanopowder was prepared from deionized water (Millipore, electrical resistivity >18 MΩ cm), totally containing 30 wt % nanoparticles. The addition of a high molecular, block-copolymeric dispersing additive with acidic, pigment-affinic groups (7 wt % relative to $Ag/CaCO_3$, Disperbyk 190, BYK Chemie) resulted in a stable dispersion after high-power ultrasonication (5 min in an ice-bath; Dr. Hielscher, UP400S, 0.4 cycle, 80% intensity). The obtained dispersion was finally filtered through a syringe filter (5 μm, Whatman).

Polymer Supported Nanoporous Silver Membranes. First, a Polysulfone (PSU) foil was prepared by roll coating (80 μm roll gap, Zehntner ZAA 2300) a PSU/Dichloromethane solution (15% PSU) on a glass substrate (20 × 15 cm), which after evaporation of the solvent resulted in a foil thickness of 10 μm. The $Ag/CaCO_3$ dispersion was then roll-coated (50 μm roll gap, 20 mm s^{-1}) on the obtained PSU foil and dried for 1 min at 170 °C. The application of the dispersion was done 3 times for a total dry film thickness of 1 μm. The coated PSU foil was then placed in an oven for 15 min at 170 °C in order to physically link silver particles by sintering. Finally, the dissolution of the calcium carbonate in 1% HCl resulted in a nanoporous silver film supported by the PSU foil.

Ag Membrane Filter. For the fabrication of a functional filter membrane, a stainless steel mesh (325 × 2300 mesh size, BOPP) was used as a mechanical support for the silver membrane. After the steel mesh was soaked with a polyimide solution (Torlon 4000, 1% in DMSO), the nanoporous silver membrane (still on the PSU foil) was attached to it. After heating the whole sandwich structure at 130 °C for 2 min, curing of the Torlon 4000 resulted in a solvent stable bonding of the silver membrane to the steel mesh. The membrane transfer was completed by dissolving the PSU substrate by washing in dichloromethane. In total, two silver membranes were transferred subsequently to the steel mesh of which the first silver membrane exhibited large pores and a lower volume porosity for a further enhancement of the mechanical stability of the second silver membrane. A 13 mm PTFE seal washer was attached to the filter by a 2-component epoxy resin (UHU). The complete filter was then placed in a plastic filter holder (Swinney filter holder, PALL).

Water volume flows were measured using a 10 mL buret where an exact filtration pressure could be applied by adjusting the water level (hydrostatic pressure). Commercial silver membranes with a nominal pore size of 0.2 μm were purchased from SPI Supplies. The filter efficiency was determined using a carbon black dispersion (black ink, BECKER) which was diluted to a total particle concentration of 10^{11} mL^{-1}. For comparison to commercial filter membranes, the same dispersion was filtered through a PTFE (0.2 μm, Macherey-Nagel, Chromafil 0-20/15MS) and a cellulose filter (0.2 μm, Whatman Spartan 13).

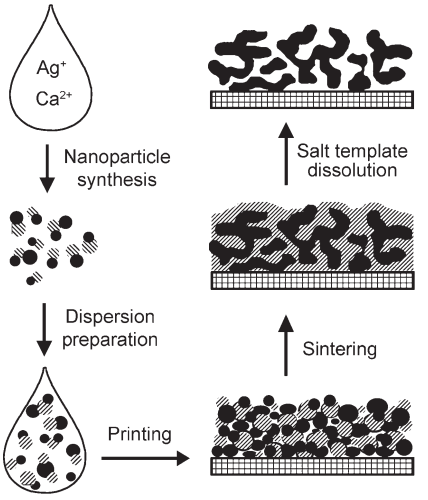

Figure 1. Schematic illustration of the Ag membrane fabrication. Starting from an organic precursor, $Ag/CaCO_3$ composite nanoparticles (dry powder) are produced by flame synthesis. After the preparation of a water-based $Ag/CaCO_3$ dispersion, the application on a substrate results in a film of homogeneously distributed Ag (= black) and $CaCO_3$ (= gray). Sintering at elevated temperature allows the cross-linking of the silver phase. After dissolution of the $CaCO_3$, the resulting membrane consists of pure silver exhibiting interconnected pores.

Analytical Methods. Scanning electron microscopy (SEM) was performed on a Leo 1530 Gemini at an accelerating voltage of 3 kV. UV−vis measurements were performed on a Shimadzu UV−visible spectrophotometer (UV-1650PC) and particle size distributions were obtained from light scattering (Nanosight, nanoparticle analysis system, LM20). Powder X-ray diffraction (XRD) was done on a Panalytical X'Pert Pro MPD (Cu K_α radiation, step size 0.3).

Results and Discussion

Figure 1 schematically illustrates the fabrication procedure: (1) Starting from an organic precursor,[20] metal/salt composite nanoparticles ($Ag/CaCO_3$) are prepared by flame synthesis;[18,21] (2) an $Ag/CaCO_3$ containing water-based dispersion is applied on a substrate (printing or roll-coating); (3) heating the metal/salt nanoparticles affords a partially sintered composite of metallic silver and calcium carbonate; (4) the salt template (i.e., $CaCO_3$) can be easily dissolved in a slightly acidic solution resulting in a pure silver membrane with interconnected pores; and (5) optional heat treatment increases the pore size of the free-standing nanoporous silver membranes (denoted as the Ag membrane).

The $Ag/CaCO_3$ composite nanoparticles[19] used here had a silver content of 80 wt % (this corresponds to 50 vol %). Other metal/salt composite nanopowders could be readily accessible considering the already broad range of previously reported, flame derived two-phase composite

(19) Madler, L.; Kammler, H. K.; Mueller, R.; Pratsinis, S. E. *J. Aerosol Sci.* **2002**, *33*, 369.

(20) Stark, W. J.; Madler, L.; Maciejewski, M.; Pratsinis, S. E.; Baiker, A. *Chem. Commun.* **2003**, 588.

(21) Athanassiou, E. K.; Krumeich, F.; Grass, R. N.; Stark, W. J. *Phys. Rev. Lett.* **2008**, 101.

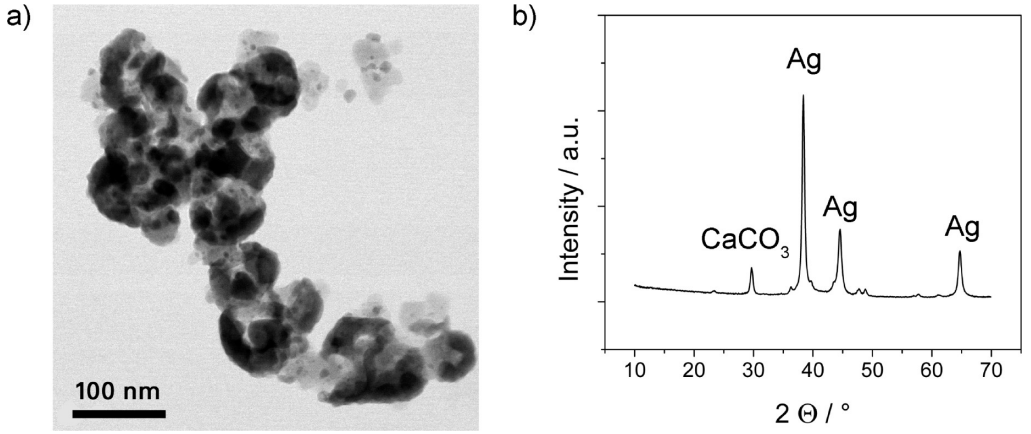

Figure 2. Transmission electron micrograph of as-prepared $Ag/CaCO_3$ nanopowders where metallic silver (dark) and calcium carbonate (light) can be clearly distinguished (a). The corresponding powder X-ray diffractogram confirms the presence of metallic silver and calcium carbonate. The use of such tightly mixed composite nanoparticles circumvents mixing problems when combining salts and metals in a material.

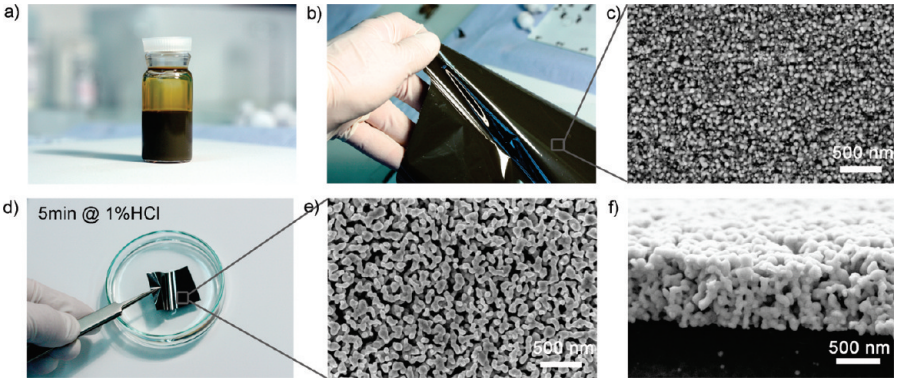

Figure 3. Fabrication of a nanoporous Ag membrane. Water based dispersion containing 30 wt % $Ag/CaCO_3$ nanoparticles (a). After applying the dispersion on a Polysulfone (PSU) foil and subsequent drying at RT (b), the resulting film contained well mixed metallic silver (light dots) and $CaCO_3$ (c). After sintering at 170 °C, the $CaCO_3$ template was dissolved in 1% HCl (d) turning the $Ag/CaCO_3$ composite film into a nanoporous Ag membrane (e). A cross-sectional view confirmed that the pores were present over the whole thickness of the membrane (f).

nanoparticles.[18,22,23] Transmission electron micrographs of the as-prepared nanopowder (Figure 2a) show two different material phases. The dark and light areas could be attributed to silver and calcium carbonate, respectively, which was further proven by powder X-ray diffractometry (Figure 2b) displaying the characteristic peaks for the individual materials (metallic Ag and $CaCO_3$).

The calcium carbonate content of the nanopowder was quantitatively determined by carbon analysis (microanalysis) resulting in 2.23 wt % C, which corresponds to 18.5 wt % $CaCO_3$. This result is in reasonable agreement with the nominal $CaCO_3$ content of 20 wt %. A stable, water-based dispersion with 30 wt % $Ag/CaCO_3$ composite nanoparticles was prepared by the use of a commercial, polymer-based dispersing agent (Disperbyk 190, 7 wt % relative to $Ag/CaCO_3$) and high-power ultrasonication (UP-400S, Hielscher Ultrasonics). The obtained dispersion was applied on a 10 μm thick polysulfone (PSU) foil by roll coating[24] and dried at room temperature (Figure 3a,b). Roll-coating was chosen as the application method of choice as it allows the homogeneous deposition of the present dispersion on a substrate. Alternatively, techniques such as inkjet printing could be used to deposit wet dispersion films with well-defined two-dimensional geometries. The resulting dry film exhibited a film thickness of around 1 μm and was composed of distributed metallic silver and $CaCO_3$ areas (Figure 3c). Subsequent sintering at 170 °C for 15 min caused the fine silver particles to cross-link, forming an interconnected silver phase. In order to create nanoporosity, the $CaCO_3$ template was removed by dissolution in 1% HCl for 5 min (Figure 3d). The pore size of the obtained nanoporous Ag membrane was < 100 nm as determined by scanning electron microscopy (SEM) (Figure 3e). A cross-section view confirms that the pores are interconnected, accessible, and present over the whole thickness of the membrane (Figure 3f). The obtained nanoporous silver membranes did not exhibit any cracks as is observed for dealloyed metals such as nanoporous gold.[25] The reason for the absence of membrane shrinking and the resultant cracking in the present system can be attributed to pore formation, which

(22) Luechinger, N. A.; Grass, R. N.; Athanassiou, E. K.; Stark, W. J. *Chem. Mater.* **2010**, *22*, 155.
(23) Huber, M.; Stark, W. J.; Loher, S.; Maciejewski, M.; Krumeich, F.; Baiker, A. *Chem. Commun.* **2005**, 648.
(24) Loher, S.; Stark, W. J.; Maienfisch, T.; Bokorny, S.; Grimm, W. *Polym. Eng. Sci.* **2006**, *46*, 1541.
(25) Parida, S.; Kramer, D.; Volkert, C. A.; Rosner, H.; Erlebacher, J.; Weissmuller, J. *Phys. Rev. Lett.* **2006**, *97*, 035504.

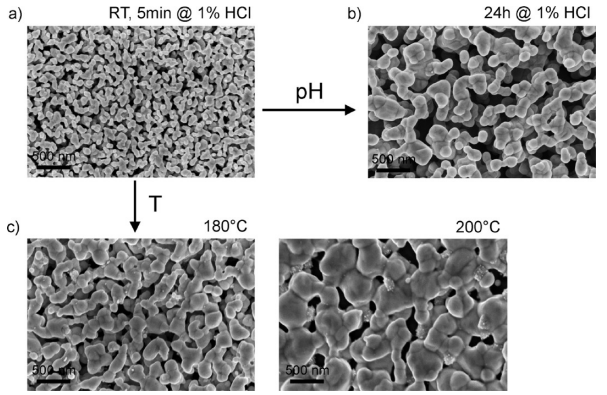

Figure 4. Manipulating the microstructure of Ag membranes. Starting from an as-prepared nanoporous Ag membrane (a), the microstructure can be tuned either by exposure to low pH or elevated temperatures. Keeping the membrane in 1% HCl for 24 h allows the silver to rearrange and reduce the totally available silver surface. The result is a larger ligament and pore size (b). When a temperature treatment is applied (sintering), the ligament size is increased, but porosity decreases due to sintering densification (c).

only involves the dissolution of the calcium carbonate template and does not require restructuring of the silver matrix.

As cracks have a dramatic negative influence on the mechanical strength of dealloyed metal membranes, in contrast, present crack-free silver membranes could be used for load-bearing applications.

The pore size could be further tuned by either exposure to low pH or elevated temperature (Figure 4). Exposing an as-prepared nanoporous Ag membrane to 1% HCl for 24 h afforded an increased average ligament size (distance between two pores) of about 200 nm. The observation of morphological changes of the silver in the presence of hydrochloric acid (HCl) has been unexpected since bulk metallic silver has been known for its low reactivity and marginal solubility in HCl (formation of nearly insoluble AgCl on the metal surface). However, this observation stays in line with findings by Li et al. who found that silver nanoparticles can indeed react with HCl and form AgCl due to size dependent standard electrode potentials.[26]

As an alternative to the pH treatment, a comparable change in ligament size could also be achieved by sintering an as-prepared membrane for 10 min at 180 °C. Both treatments (pH or thermal) are thermodynamically driven (minimization of total internal surface energy by reducing the specific surface area) and indicate a significant mobility of silver atoms in the present material. In the case of a temperature treatment, surface- and bulk diffusion of silver atoms are increased allowing grain coarsening (larger ligament size) and sintering densification (lower porosity). It is known from solid state sintering theory that sintering densification only takes place if bulk atom diffusion is activated.[27] Since a pH treatment only involves reactions ($2Ag + 2HCl \rightarrow 2AgCl + H_2$; $Ag^{\alpha}Cl + Ag^{\beta} \rightarrow Ag^{\alpha} + Ag^{\beta}Cl$, where α and β denote two different silver atoms, and Ag^{α} is reduced by Ag^{β}) and diffusion of silver surface atoms, in contrast to the temperature treatment, no significant densification (porosity loss) could be observed (Figure 4b).

A notable difference between the present Ag membrane and dealloyed metals is the average grain size. Metals made by dealloying exhibit a grain size of several tens of micrometers (grain size $\gg$ ligament size) because the dealloying mechanism is independent of grain boundaries. This is different for the Ag membrane prepared here since the building blocks, Ag nanoparticles, are individual grains (see XRD-pattern in Figure 2b) with different crystallographic orientations. Therefore, the grain size in as-prepared Ag membranes is similar to the ligament size of around 100 nm (Figure 4a).

Nanoporous metals made by dealloying exhibit macrodefects in the form of cracks. This is attributed to the large volume shrinkage (up to 30%) during dealloying which is an obvious cause of cracking. The silver membranes presented here are defect and crack-free since during pore formation (removal of $CaCO_3$ template), no volume shrinkage occurs (Figure 5c). This allows new applications where defect-free materials are essential. In filtration for instance, only intact membranes will guarantee a reliable performance. We have therefore investigated the technical feasibility of using a nanoporous silver membrane for nanofiltration.

Figure 5 shows the assembly of a nanofiltration membrane supported on a stainless steel mesh for mechanical stability (Figure 5a). Subsequently, two Ag membranes were transferred (Figure 5b) from the PSU foil to the steel mesh by dissolving the primary PSU support in dichloromethane. The first membrane was annealed at 200 °C for 10 min (Figure 4c) providing enhanced mechanical stability through larger ligaments and lower porosity. The second membrane was transferred as prepared (Figure 4a) and served as an effective filtration membrane. A low-magnification scanning electron micrograph shows a defect and crack-free surface of the transferred nanoporous silver membrane (Figure 4c). The first silver membrane (support membrane) was attached to the steel mesh support by a polyimide solution resulting in Ag/steel bonding areas which can be seen in the topography of Figure 5a (top view) and Figure 5d (bottom view; Ag membrane detached from steel mesh). The resulting sandwich structure consisting of the steel mesh and two silver membranes was finally shaped to fit into a polypropylene syringe filter holder (Figure 5e) after the PTFE sealing ring was attached by epoxy resin (Figure 5f).

The pore size distribution of an as-prepared Ag membrane was determined by measuring 153 arbitrarily chosen pores in scanning electron micrographs (Figure 6a). Pores ranged from 20−110 nm with a mean pore size of around 45 nm. Prior to filtration studies, the prepared filtration membrane was tested for pressure dependent flow capacity using pure water (Figure 6b). Before testing, the silver membranes were prewetted using isopropanol. The water volume flow linearly increased with pressure, which is in agreement with Hagen Poiseuille's relationship describing pressure dependent volume flow for one capillary with a certain pore size and length. If we consider the

(26) Li, L.; Zhu, Y. J. *J. Colloid Interface Sci.* **2006**, *303*, 415.
(27) German, R. M. *Sintering Theory and Practice*; John Wiley & Sons: New York, 1996.

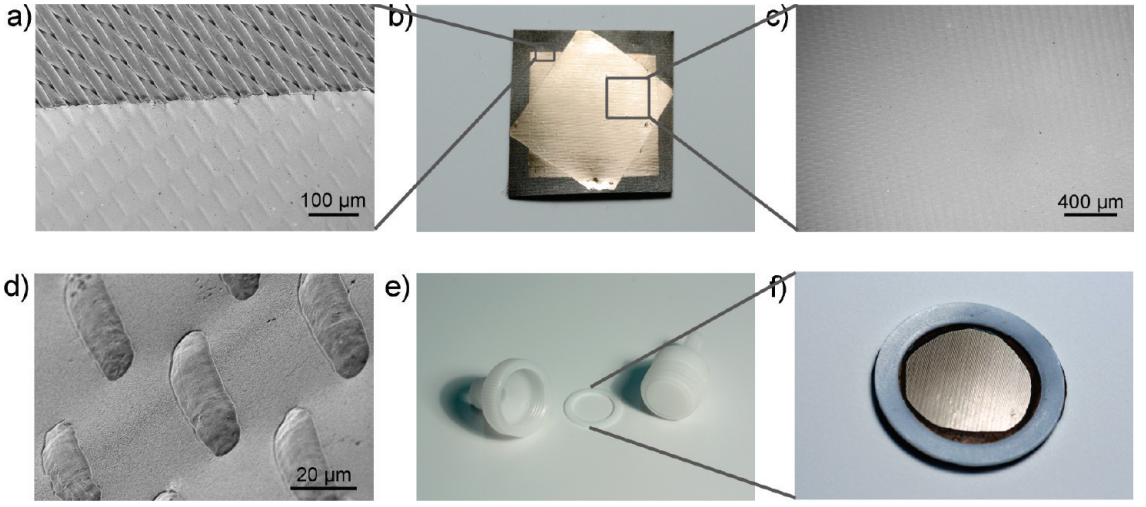

Figure 5. Fabrication of a filter membrane. Pictures of stainless steel mesh supported nanoporous Ag membranes (a,b). For enhanced mechanical stability, two Ag membranes were used where the first one was annealed at 200 °C for 10 min (see Figure 4c) (b). Scanning electron micrographs showing the defect and crack-free surface of the transferred Ag membrane (c). A membrane which was detached from the steel mesh for investigation of the polyimide Ag/steel contact areas (d). Swinney syringe filter holder (e) and PTFE sealing ring attached to the fully assembled filter membrane by epoxy resin (f).

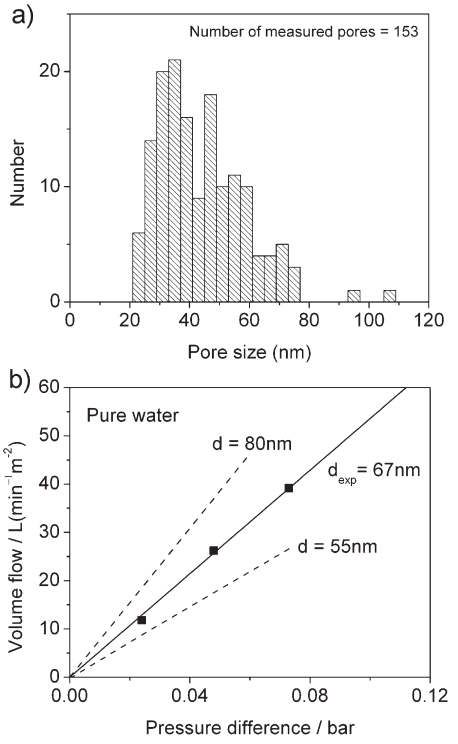

Figure 6. Pore size distribution of an as-prepared Ag membrane determined by optical evaluation of scanning electron micrographs (a). Measured liquid volume flow through the Ag membrane filter in the case of deionized water (b). Theoretical volume flows for different mean pore sizes (dashed lines) using Hagen Poiseuille's relationship and comparison to experimental values (squares).

present porous membrane to consist of a certain number of equally sized cylindrical capillaries, then Hagen Poiseuille's relationship can be written as:

$$V = \frac{A\varphi d^2 \Delta p}{32\eta t} \quad (1)$$

with volume flow V ($m^3\ s^{-1}$), area porosity φ (%), pore size d (m), differential pressure Δp (Pa), viscosity η (Pa s), and the membrane thickness t (m). We have set the length of the cylindrical capillaries of our model equal to the membrane thickness, although, due to the tortuosity of the capillaries, the real flow path would be longer, which would result in a higher calculated pore size. We made this simplified assumption as it is expected that the volume flow is larger in interconnected pores of the present membranes compared to that in the isolated cylinders of the model, which is supposed to compensate the influence of assuming a shorter capillary length. The area porosity of the silver membrane was determined as 43% by numerical image analysis of a scanning electron micrograph (see Supporting Information S1). If eq 1 is rearranged, a theoretical mean pore size can be calculated from the measured liquid volume flows (e.g., water flow at 0.1 bar pressure). A calculated pore size of 67 nm for the investigated membrane here is slightly higher than the optically determined mean pore size of 45 nm obtained from scanning electron micrographs (Figure 6a). The higher value for the calculated pore size probably results from the model assumption of equally sized capillaries. Since the volume flow depends on the square of the pore size, large pores in the size distribution will have a stronger influence compared to small ones.

Table 1. Comparison to a Commercial Ag-Membrane with the Smallest Available Pore Size

Ag membrane	nominal pore size (nm)	thickness (μm)	specific water volume flow ($l\ min^{-1}\ m^{-2}\ bar^{-1}$)
commercial	200 [a]	50 [a]	243 [a]
this work	< 80	1	534

[a] Supplier information (SPI Supplies).

Porous silver membranes have already been fabricated and commercially used since 1950. Today, numerous technical processes use these silver membranes with a thickness of 50 μm and different pore sizes (0.2 μm–5 μm). As a reference to the prepared filtration membrane here, we investigated the commercial membranes with the

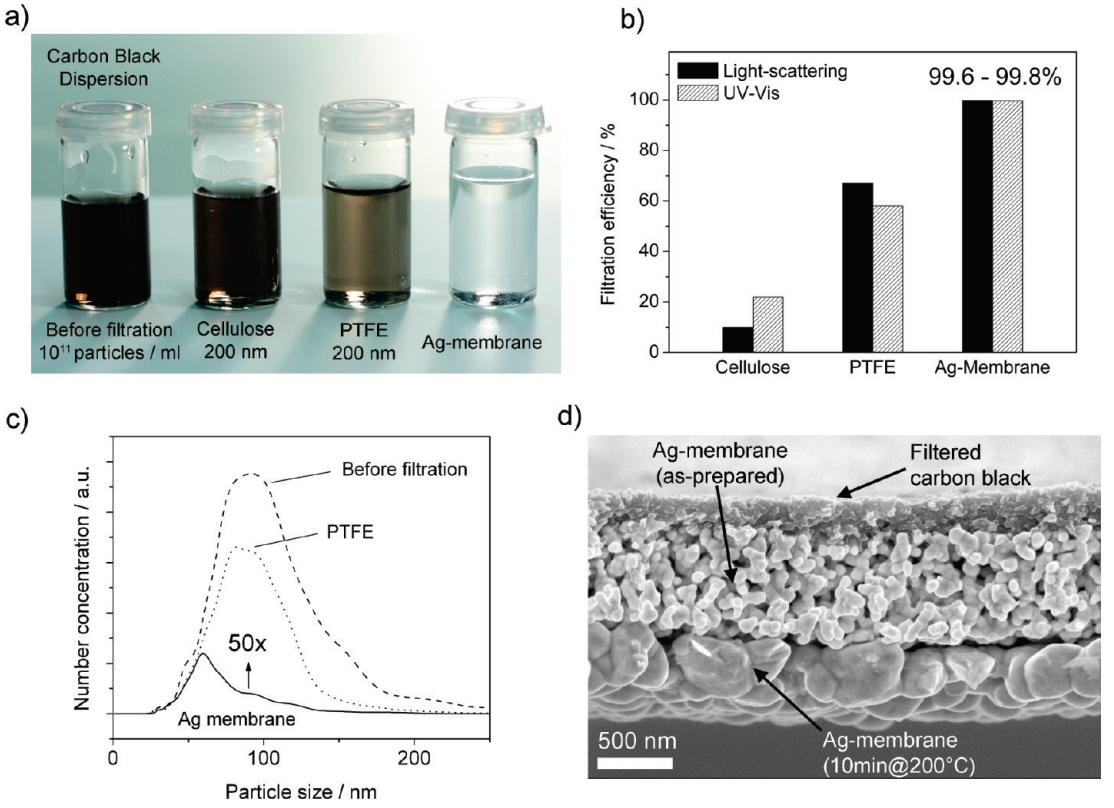

Figure 7. Filtration of carbon black colloidal nanoparticles. Test liquid based on carbon black before and after filtration through different filters (a). Filtration efficiencies of the different filters determined by UV−vis and light scattering (b). Influence of the different filters on the particle size distribution of the filtered liquids (c). Cross-section of a scanning electron micrograph of a used Ag membrane filter showing the effective filtering membrane on a supporting temperature treated Ag membrane (d). Retained carbon black particles appear as a filter cake on top of the filtering membrane.

smallest available nominal pore size of 0.2 μm by scanning electron microscopy (Supporting Information, Figure S2). For comparison, Table 1 summarizes filtration specific properties of the nanoporous Ag membrane (this work) and the reference. The specific water volume flows of both membranes are in the same range (243 L min^{-1} m^{-2} bar^{-1} compared to 543 L min^{-1} m^{-2} bar^{-1}), even though the pore size of the nanoporous silver membrane shown here is much smaller (note that the volume flow depends on the square of the pore size; eq 1). The high volume flow of the nanoporous Ag membrane is the result of the significantly higher porosity and much lower membrane thickness (50 times thinner) when compared to those of the presently available membranes.

For nanofiltration performance studies of the assembled Ag membrane filter, a test liquid was used based on a diluted black ink containing 10^{11} colloidal carbon black particles per mL (Figure 7a) as a model for typical nanoparticle containing streams. For comparison, two additional, commercial syringe filters (hydrophobic PTFE and hydrophilic cellulose) with a nominal pore size of 200 nm were compared to the Ag membrane filter shown here. After passing the test liquid through the different filters, the filtered liquids (Figure 7a) were tested for the concentration of residual carbon black particles. Concentration changes between the test liquids and the filtered liquids were determined both by UV−vis absorbance measurements and light scattering. Both analysis methods resulted in consistent filtration efficiencies and revealed that almost all carbon black particles could pass the cellulose filter (retention $<25\%$), whereas the PTFE filter retained more than 50% (Figure 7b). Unfortunately, a performance of 50% retention is insufficient for most filtration applications with nanoparticles. In contrast, the Ag membrane filter exhibited a filtration efficiency above 99.6%, which can be attributed to the significantly smaller pore size when compared to the that of commercial syringe filters. For each filter, the test liquids and filtered liquids were also compared regarding particle size distribution determined by light scattering (Figure 7c). The test liquid before filtration exhibited a particle size distribution of 25−200 nm. It can be seen in the distribution of the PTFE filtered liquid that particles larger than around 150 nm could not pass the filter. For the Ag membrane filter, the filtered liquid showed a narrowed particle size distribution of much lower concentration. The maximum was shifted from initially 90 to around 55 nm. Most of the particles which passed the Ag membrane filter had a size of 25−100 nm, which is in agreement with the measured pore size distribution in Figure 6a. After the filtration experiments, the cross-section of the Ag membrane filter was investigated by scanning electron microscopy (Figure 7d). It can be clearly distinguished between the effective filter membrane and the supporting temperature treated membrane. The retained/filtered carbon black particles appear as a filter cake on top of the filter membrane.

In summary, we have presented a method to fabricate nanoporous silver membranes by a simple approach

using soluble salt nanoparticles as a pore forming template. The present silver membranes can easily be applied on virtually any substrate material by using established technologies such as printing, roll coating, or spraying. As the template removal affords no volume shrinkage, the resulting nanoporous membranes are crack-free and allow rapid large scale manufacturing. The assembly of an integral Ag membrane filter illustrated how liquid filtering with 1 μm metal membranes is possible at high volume flow rates. Next to water treatment, nanoparticle removal and process water sterilization in biotechnology or medical applications, the properties found here are amenable to cross-flow electro-ultrafiltration where the filtering membrane also functions as an electrode.[28] The combination of electrical conductivity, high porosity, and gas permeability is further attractive for electro-catalysis and fuel cell electrodes. Since metal/salt nanoparticles have become readily available, other material pairs open fascinating opportunities for porous metal preparation well beyond the example shown here of nanoporous silver.

(28) Huotari, H. M.; Huisman, I. H.; Tragardh, G. *J. Membr. Sci.* **1999**, *156*, 49.

Acknowledgment. We acknowledge the financial support by ETH Zurich and Swiss National Science Foundation (SNF 200021-116123) as well as the electron microscopy center at ETH Zurich (EMEZ).

Supporting Information Available: Scanning electron micrograph for the determination of area porosity by numerical image analysis (Figure S1) and scanning electron micrographs of a commercial silver membrane having a nominal pore size of 0.2 μm (supplier information) and the Ag membrane (Figure S2) shown here (PDF). This material is available free of charge via the Internet at http://pubs.acs.org.